Science Translational Medicine
AAAS

www.sciencetranslationalmedicine.org/cgi/content/full/9/384/eaai8504/DC1

Supplementary Materials for

Transient tissue priming via ROCK inhibition uncouples pancreatic cancer progression, sensitivity to chemotherapy, and metastasis

Claire Vennin, Venessa T. Chin, Sean C. Warren, Morghan C. Lucas, David Herrmann, Astrid Magenau, Pauline Melenec, Stacey N. Walters, Gonzalo del Monte-Nieto, James R. W. Conway, Max Nobis, Amr H. Allam, Rachael A. McCloy, Nicola Currey, Mark Pinese, Alice Boulghourjian, Anaiis Zaratzian, Arne A. S. Adam, Celine Heu, Adnan M. Nagrial, Angela Chou, Angela Steinmann, Alison Drury, Danielle Froio, Marc Giry-Laterriere, Nathanial L. E. Harris, Tri Phan, Rohit Jain, Wolfgang Weninger, Ewan J. McGhee, Renee Whan, Amber L. Johns, Jaswinder S. Samra, Lorraine Chantrill, Anthony J. Gill, Maija Kohonen-Corish, Richard P. Harvey, Andrew V. Biankin; Australian Pancreatic Cancer Genome Initiative (APGI), T. R. Jeffry Evans, Kurt I. Anderson, Shane T. Grey, Christopher J. Ormandy, David Gallego-Ortega, Yingxiao Wang, Michael S. Samuel, Owen J. Sansom, Andrew Burgess, Thomas R. Cox, Jennifer P. Morton, Marina Pajic*, Paul Timpson*

*Corresponding author. Email: m.pajic@garvan.org.au (M. Pajic); p.timpson@garvan.org.au (P.T.)

Published 5 April 2017, *Sci. Transl. Med.* **9**, eaai8504 (2017)
DOI: 10.1126/scitranslmed.aai8504

The PDF file includes:

Other Supplementary Material for this manuscript includes the following:
(available at www.sciencetranslationalmedicine.org/cgi/content/full/9/384/eaai8504/DC1)

Movie S1 (.mp4 format). 4D monitoring of fibroblast-ECM interactions upon treatment with vehicle and Fasudil.
Movie S2 (.mp4 format). Live FLIM-FRET imaging of the CDK1 biosensor in KPC cells in response to Abraxane and Abraxane + RO3306.
Movie S3 (.mp4 format). Live FLIM-FRET imaging of the CDK1 biosensor in KPC cells in interphase and mitosis.
Movie S4 (.mp4 format). Live FLIM-FRET monitoring of CDK1 activity in KPC cells actively interacting with an organotypic matrix.
Movie S5 (.avi format). Intravital FLIM-FRET imaging of subcutaneous xenografts with KPC-CDK1 cells and imaging of fibrillar collagen.
Movie S6 (.mp4 format). Intravital monitoring of CDK1 accumulation in subcutaneous KPC tumors.
Movie S7 (.mp4 format). Intravital imaging of quantum dots circulating through tumor-associated vasculature and diffusing into tumor tissue upon priming with Fasudil.
Movie S8 (.mp4 format). Imaging of liver tissue with metastatic KPC cells expressing the CDK1 biosensor forming macrometastases and micrometastases.
Movie S9 (.mp4 format). Time-lapse tracking of collective cell streaming on CDMs unprimed or primed with Fasudil.

Materials and Methods

Animals. Animal experiments were conducted in accordance with the Australian code of practice for the care and use of animals for scientific purposes and in compliance with Garvan Ethics Committee guidelines (13/17, 14/06, 14/11, and 16/13 protocols).

Drug treatment. Fasudil (HA-1077, Jomar Life Research) was administered by oral gavage every 12 hours for 3 days in saline buffer (100 mg/kg). In the subcutaneous xenograft model, priming started when average tumor volume reached 180 mm^3. Specifically, day 1 of priming was on day 6 after injection of KPC-CDK1 cells, on day 21 after injection of TKCC5-CDK1 cells, and on day 9 after injection of TKCC2-CDK1 cells. In the intrasplenic model, mice were subjected to three priming treatments with Fasudil before intrasplenic injection of KPC-CDK1 cells and to three subsequent priming treatments with Fasudil after intrasplenic injection of KPC-CDK1 cells. In the orthotopic model, the first priming treatment with Fasudil started on day 3 after injection of TKCC5-Luciferase cells, when tumors were established as assessed by IVIS monitoring (average luciferase total flux signal: 5 x 10^7 p/s). In vitro, Fasudil was used at 5 μM in cell culture medium. Abraxane (Specialized Therapeutics, 30 mg/kg) and gemcitabine (Jomar Life Research, 70 mg/kg) were administered by intraperitoneal injection (or 100 nM in cell culture medium in vitro). Y-27632 (Selleckchem, 10 μM) and RO3306 (Axon MedChem, 10 μM) were used in cell culture medium in vitro.

Cell culture. Primary KPC cancer cells were isolated from *Pdx1-Cre, LSL-KRas$^{G12D/+}$, LSL-Trp53$^{R172H/+}$* tumors (*13*). Telomerase-immortalized fibroblasts (TIFs) were generated as previously described (*79*). Human cancer cells and activated cancer-associated fibroblasts (CAFs) were isolated from patient-derived xenografts as previously described (*18*). Cancer cells were engineered to express the mCerulean-YFP CDK1 FRET biosensor (*14, 15*) using a 3rd generation lentiviral packaging system, and the mTurquoise2-YPet SRC-FRET biosensor (*48*) was introduced using a transposon system (see details below). KPC cells and TIFs were cultured in DMEM (Gibco) complemented with 10% FBS and 1% penicillin/streptomycin in 20% O_2/5% CO_2. TKCC5 cells were cultured in transformed HPAC (Gibco) medium, and TKCC2 cells were cultured in RPMI (Gibco) in 20% O_2/5% CO_2. CAFs from TKCC5 and TKCC2 PDXs and cancer cells from TKCC2 PDX were cultured in 5% O_2/5% CO_2, while cancer cells from TKCC5 PDX were cultured in 20% O_2/5% CO_2 conditions.

Generation of KPC cell line expressing the SRC-FRET biosensor. For stable expression of the SRC-FRET biosensor, cells were co-transfected with a pPB.DEST-SRC vector and pCMV-hyPBase (obtained

from the Wellcome Trust Sanger Institute) (*80*). To generate the pPB.DEST vector, the gateway cassette from pEF-DEST51 (ThermoFisher Scientific) was PCR-amplified using the primers 5' - CATCGATGATCAACCACTTTGTACAAGAAAGC - 3' and 5' – CCTCGAGAAGCTTGATCAACAAGTTTGTACAAAAAAGCTG - 3'. This cassette was then inserted into the EBNXN site of pPB-CAG.EBNXN (also obtained from the Wellcome Trust Sanger Institute (*81*)) using the ClaI and XhoI restriction sites. To move the SRC-FRET biosensor into the pPB.DEST vector, it was first subcloned from pcDNA3.1 into pENTR2b using the HincII and PmeI restriction enzymes, then an LR reaction (LR clonase II, ThermoFisher Scientific) was performed to create pPB.DEST-SRC.

Organotypic assays. Organotypic assays were conducted as previously described (*82-84*). Rat tail tendon collagen was extracted with 0.5 mM acetic acid to a concentration of 2.5 mg/ml. $8.4x10^4$ TIFs or $2x10^5$ CAFs were embedded in 2.5 ml of rat-tail collagen I. Once polymerized, fibroblast-collagen matrices were allowed to contract in DMEM containing 10% FBS and 1% penicillin/streptomycin until the fibroblasts had contracted the matrix (12-day contraction for the TIFs, 7-day contraction for the CAFs). TIFs-driven contraction consistently reached saturation by day 10 of contraction. After contraction, $4x10^4$ cancer cells were seeded on the contracted matrix in complete medium and allowed to grow to confluence for 4 days. The matrix was then transferred to a metal grid and raised to an air-liquid interface. KPC cells invaded for 12 days, TKCC5 cells invaded for 15 days, and TKCC2 grew for 21 days with a medium change every 2 days. For drug treatment, 5 μM Fasudil or 10 μM Y-27632 were added to the medium during contraction and renewed at day 6; 5 μM Fasudil was added to the medium below the matrix throughout the invasion period (renewed every two days); 100 nM gemcitabine and 100 nM Abraxane were added to the medium below the metal grid for 72 hours at the end of the invasion phase. After invasion, organotypic matrices were imaged or fixed in 10% formalin and processed for histochemistry analysis. Invasive index was measured in 3 representative areas per matrix as per the formula:

$$Invasive\ index = \frac{Number\ of\ invading\ cells}{(Number\ of\ invading\ cells + number\ of\ non-invading\ cells)} \times 100$$

SHG imaging and analysis. SHG signal was acquired using a 25x 0.95 NA water objective on an inverted Leica DMI 6000 SP8 confocal microscope. Excitation source was a Ti:Sapphire femtosecond laser cavity (Coherent Chameleon Ultra II), operating at 80 MHz and tuned to a wavelength of 840 nm or 920 nm. Intensity was recorded with RLD HyD detectors (420/40 nm or 460/20 nm, respectively). For each sample, 3 representative regions of interest of 512 μm x 512 μm were imaged over a 3D z-stack (80 μm depth for organotypic matrix with a z-step size of 2.52 μm; 20 μm depth for CDMs, xenografts, and

liver tissue with a z-step size of 1.5 μm). SHG imaging of organotypic matrices was performed on formalin-fixed samples and on 20-μm thick H&E sections for xenograft and liver tissues. The intensity of the SHG signal was measured with ImageJ (US National Institutes of Health). Representative images of maximum intensity projections are shown.

Polarized light microscopy and analysis. 4 μm sections of fixed samples were deparaffinized, rehydrated, and stained with 0.1% picrosirius red (Polysciences) for fibrillar collagen according to manufacturer's instructions. Polarized light images were collected using an Olympus U-POT polarizer in combination with an Olympus U-ANT transmitted light analyzer fitted to the microscope. Quantitative intensity measurements of fibrillar collagen birefringent signal were carried out on polarized light images using ImageJ. For each polarized light image, Hue-Saturation-Balance (HSB) thresholding was applied, where $0 \geq H \leq 29$ | $0 \geq S \leq 255$ | $70 \geq B \leq 255$ was used for red-orange (high birefringent) fibers, $30 \geq H \leq 44$ | $0 \geq S \leq 255$ | $70 \geq B \leq 255$ for yellow (medium birefringent) fibers, and $45 \geq H \leq 245$ | $0 \geq S \leq 255$ | $70 \geq B \leq 255$ for green (low birefringent) fibers. The relative area (as a % of total fibers [$0 \geq H \leq 245$ | $0 \geq S \leq 255$ | $70 \geq B \leq 255$]) was then calculated.

Live imaging of fibroblast-collagen matrix and cancer cells on cell-derived matrix. Imaging was performed using the system described above (SHG imaging). Samples were placed in a humidified heated chamber (37˚C, 5% CO_2) and z-stacks were acquired every 20 min for 8 hours. For dual imaging of GFP-fibroblasts and collagen I, excitation wavelength was 890 nm to simultaneously acquire GFP signal (525/50 nm) and SHG signal (440/20 nm). KPC-CDK1 cells seeded on CDMs were imaged using a centered wavelength of 840 nm and a 490/40 nm filter. Image stack time-series were reconstructed with Imaris 8 (Bitplane) and presented as maximum intensity projections. Protrusion number, average length and persistence, and cell circularity were quantified manually in ImageJ software (US National Institutes of Health). Fibroblasts in collagen matrix were imaged at day 6 of contraction; KPC cells were imaged 24 hours after seeding on CDMs.

Gray-level co-occurrence matrix. Stromal collagen fiber organization and crosslinking were assessed using gray-level co-occurrence matrix (GLCM) analysis. This method allows characterizing the texture of a sample and determines the correlation of the SHG signal within the matrix (*23*). The correlation plots represent the similarity in signal strength between pixels. A slower decay shows a more organized and correlated network of collagen fibers than in samples with a faster decay. GLCM analysis was performed in ImageJ (US National Institutes of Health). First, the user selected a directory containing three

representative single-plane SHG images for each sample. SHG signal of similar intensity and with a line average of 16 was acquired for each sample for accurate quantification of collagen fiber organization. The average texture parameter for each image was calculated using looped operation of the plug-in and for 0°, 90°, 180° and 270° directions. Normalized texture parameters were calculated in MATLAB (MathWorks) for each image, and the mean correlation along with the SEM was imported and plotted against the neighbor index in GraphPad software.

Scanning electron microscopy (SEM) of fibroblast-collagen matrix. A JEOL 6490LV scanning electron microscope equipped with a secondary electron (SE) detector and a backscattered electron (BSE) detector (scintillator type) was used at acceleration voltages between 10 and 20 kV. Images were recorded with an integrated JEOL digital image acquisition system. Before SEM imaging, samples were sliced and clamped in a cooling holder, plunged into a bath of liquid nitrogen for 45 seconds, and then fractured with a liquid nitrogen cooled blade.

Atomic force microscopy (AFM) measurement of matrix stiffness. Organotypic matrices were immobilized on a 40 mm glass bottom cell culture dish using a 10% agarose solution (Bioline Australia). A Bioscope Catalyst (Bruker) mounted on a TMC anti-vibration table (Technical Manufacturing Corporation) was used for nano-indentation. Measurements were performed using a 1 μm spherical colloidal probe (Novascan) with a spring constant of 0.06 N/m mounted on the fluid holder of the AFM scanner. AFM calibration was achieved by measuring the deflection sensitivity of the probe in fluid by engaging the probe on an uncoated glass substrate, withdrawal of the probe, and then using a thermal tune sweep to determine the spring constant. Indentation was performed using a peak force tapping mode (average loading force of 1 nN) on 4 different areas per matrix and 30 indentation points per area. The Young's modulus values were calculated from force curves using the Hertz spherical indentation model (*85*).

Immunoblotting. Cells were lysed in protein extraction buffer (50 mM HEPES, 1% Triton-X-100, 0.5% sodium deoxycholate, 0.1% SDS, 0.5 mM EDTA, 50 mM NaF, 10 mM Na_3VO_4, and protease cocktail inhibitor (Roche)) or in NP40 extraction buffer (150 mM sodium chloride, 1% NP-40, 50 mM Tris pH 8). Lysates were separated by 10% acrylamide Bis-Tris gel electrophoresis, and proteins were transferred onto a PVDF membrane (Immobilon-P, Millipore), blocked with 5% milk or BSA buffer, incubated with primary antibodies overnight at 4^0C, and probed with HRP-linked secondary antibodies (GE Healthcare, 1:5,000 diluted in 1% milk). Signal was detected using ECL reagent (Pierce on X-ray films (Fujifilm)).

Signal was normalized to β-actin signal.

Proliferation assay. 1,000 KPC cells/well were plated in a 96-well microtiter plate and incubated for 24 hours to allow attachment. On day 0, cells were treated with gemcitabine and Abraxane. Cell proliferation was determined at day 3 and day 5 using the CellTiter 96 aqueous assay (Promega) in accordance with manufacturer's protocol and normalized to day 0 after blank correction.

DNA FACS analysis. Cells were fixed in 70% ethanol, stained with propidium iodide, and then analyzed on FACS Canto II (BD Bioscience).

Immunofluorescence staining of β-tubulin. Cells were seeded on glass coverslips and fixed in PHEM buffer (25 mM HEPES, 10 mM EGTA, 60 mM PIPES, and 2 mM $MgCl_2$). Cells were permeabilized using Triton-X-100 (0.5% in PHEM buffer, 1 min). Subsequently, cells were blocked with BSA for 30 min and incubated with anti-β-tubulin (1:50) overnight at 4^0C. Cells were incubated with Alexa488-coupled secondary antibody (Jackon ImmunoResearch Laboratories Inc.), counter-stained with DAPI, and mounted in Mowiol mounting medium.

FLIM-FRET imaging and analysis. For in vivo measurements of mCerulean and mTurquoise2 lifetimes in live tissues, cancer cells expressing the CDK1-FRET biosensor or the SRC-FRET biosensor were trypsinized and resuspended in cold phosphate-buffered saline (PBS). $1x10^6$ cells were injected subcutaneously into the rear flank and $5x10^5$ cells were injected into the spleen of BALB/c-Fox1nuAusb mice under anesthesia (isoflurane 3 L, O_2 1 L/min, vacuum was used constantly to remove excess of O_2). Before imaging, mice were anesthetized using a mix of 10 mg/kg xylazine, 50 mg/kg tiletamine and 50 mg/kg zolazepam. Subcutaneous tumors were surgically exposed for intravital imaging as previously described (*84*), and the mouse was maintained under anesthesia (isoflurane 3 L, O_2 1 L/min, vacuum was used constantly to remove excess of O_2) while placed and restrained on a 37°C stage. For imaging of liver metastases, mice were euthanized, and fresh organs were harvested and immediately imaged (imaging duration <45 min after euthanasia). Imaging was performed using the system described above (SHG imaging). mCerulean was excited at 840 nm, and the signal was detected using a 490/40 nm filter; mTurquoise2 was excited at 840 nm, and signal was detected using a 483/40 nm filter. FLIM data were recorded using a Picoharp 300 TCSPC system (Picoquant). Images of 512 x 512 pixels were acquired with a line rate of 600 Hz. The pixel dwell time was 5 μs, and images were integrated until 700 photons per pixel were acquired. mCerulean and mTurquoise2 lifetimes were analyzed by drawing ROIs around

subcellular areas and recording the lifetime (τ) of the single exponential function fit to the fluorescence decay data. Lifetime maps were generated with intensity thresholds set to the average background pixel value for each recording. The raw data were smoothed, and a standard rainbow color look up table (LUT) was applied, with lifetimes of 1.6 ns to 3.2 ns for mCerulean and 2 ns to 4 ns for mTurquoise2. Areas where no lifetime measurement above the background noise could be achieved are shown in black in the lifetime map.

Quantum Dot imaging and quantification. $1x10^6$ cells were injected subcutaneously into the rear flank of BALB/c-Fox1nuAusb mice under anesthesia (isoflurane 3 L, O_2 1 L/min, vacuum was used constantly to remove excess of O_2). From day 6, mice were primed with Fasudil (oral gavage, 100 mg/kg, twice daily treatment) for three days. At day 11 after KPC cell injection, when chemotherapy was initially administered, 100 µl of QTracker 655 nm (20 nm diameter, 500 kDa; 1:10 dilution in PBS, Life Technology) was administered via intravenous injection 10 min before imaging, as previously achieved (*84*). Mice were subsequently anesthetized using a mix of 10 mg/kg xylazine, 50 mg/kg tiletamine and 50 mg/kg zolazepam. Subcutaneous tumors were surgically exposed for intravital imaging, and the mice maintained under anesthesia (isoflurane 3 L, O_2 1 L/min, vacuum was used constantly to remove excess of O_2) were placed and restrained on a 37°C stage. Quantum Dots were excited at 920 nm, and signal was collected using a 650/20 nm filter. For each mouse, 10 representative regions of interest of 512 µm x 512 µm were imaged over a 3D z-stack. Quantification of Quantum Dot signal inside and outside blood vessels was performed as follows. 3D z-stacks were converted to maximum intensity projections in ImageJ. The ratio of the Qtracker signal inside versus outside of vessels was quantified by manually outlining blood vessels and applying an intensity threshold. The intensity was measured inside and outside blood vessels, and the ratio of intensity outside versus inside was calculated. A high ratio indicated a high degree of leakiness, whereas a low ratio showed that vessels remained intact and Qdots did not leak into the surrounding tissue.

Intrasplenic and orthotopic injections of cancer cells. For intrasplenic injection experiments, KPC cells ($5x10^5$ cells/50 µL PBS) were injected into the spleens of BALB/c-Fox1nuAusb mice (anesthetized with isoflurane 3 L, O_2 1 L/min, vacuum was used constantly to remove excess of O_2) as previously described (*86*), and liver metastases were imaged 10 days after intrasplenic injection. For the survival experiment using orthotopic injection, NOD/SCID/ILR2γ mice were anesthetized (isoflurane 3 L, O_2 1 L/min, vacuum was used constantly to remove excess of O_2), and TKCC5 cells ($5x10^3$ cells/50 µL PBS/Matrigel (1:1) mix) were injected into the pancreas during open laparotomy. For the intrasplenic

injection experiment, mice were subjected to three rounds of priming with Fasudil by oral gavage before intrasplenic injection, and three subsequent rounds of priming with Fasudil to mimic systemic ROCK inhibition during metastatic spread of KPC cells (twice daily administration by oral gavage). Mice were then treated with gemcitabine and Abraxane on days 7, 8, and 9 after injection. See Fig. 5A for treatment timeline details. For the orthotopic tumor experiment, the treatment cycle started on day 3 after injection, when the tumors were established according to IVIS monitoring (average luciferase IVIS total flux signal = 5 x 10^7 p/s). Experimental endpoints were development of ascites, overnight weight loss >10% of body weight, or hunching posture and signs of pain. See Fig. 8F for details of the treatment timeline.

Quantification of microvessels and capillaries in the liver. Morphometric quantification was performed using the Amira 6 software (FEI, Thermo Scientific). CD31 stained/hematoxylin counterstained liver sections were used for quantification. After light inversion performed in Photoshop (Adobe), images were saved and opened in Amira 6. Images underwent segmentation using a combination of automatic and manual selections available in the software (see Fig. S4A for representative images of segmentation). During segmentation, capillary and vessel endothelium, capillary lumen, vessel lumen, and the rest of the tissue were separated into different selections for area and object quantification. The final number of objects was normalized to the total area of tissue quantified in the image.

Quantification of liver metastases. Total number of liver metastases, extravasation events, and emboli morphology were quantified on serial sections (5 sections per organ with a 100 μm step). The area covered by the whole liver tissue was measured with ImageJ (US National Institutes of Health). Extravasation events were defined as clusters of KPC cells (>8 cells, PDX-1+) that breached through the matrix surrounding blood vessels (Elastica Van Gieson staining, confirmed by A.J.G., a trained pathologist and co-author of the manuscript). All blood vessels were considered for quantification. For analysis of metastatic emboli morphology, lines of aligned KPC cells (PDX-1+) either sprouting from metastases or aligned in the liver tissue and disconnected from round metastases were quantified in comparison to round, individual metastases.

Cell-derived matrix (CDM) assay. CDMs were established as previously described (*40*). For priming, Fasudil was added to the medium at day 0 of matrix production and renewed at day 4, and ascorbic acid (50 μg/ml) was added to the medium every two days. Fibroblasts were removed at day 7, and CDMs were washed three times before seeding of 4x10^4 KPC cells. Cell adhesion was monitored for 48 hours on a

live cell microscope (Leica DMI 6000) with a 10x objective. To quantify cell adhesion onto CDMs, differential interference contrast (DIC) images were acquired every hour. The images were locally background subtracted using a 25px radius filter. Variance images were calculated by computing the local variance in an 8px radius region. Cell area coverage was computed by thresholding the variance image to identify cells. Also see script below.

```
function [coverage,mask] = ComputeCellCoverage(im)
   % Script to compute cell coverage from DIC images
   % Threshold should be set appropriately

   % Perform background subtraction
   ksize = 25;
   k = fspecial('disk',ksize);
   bf = conv2(im,k,'same');
   bgsub = im-bf;

   % Crop to central valid region
   bgsub = bgsub(ksize:(end-ksize),ksize:(end-ksize));
   ksize = 3;
   bgsub = medfilt2(bgsub,[ksize, ksize]);

   % Compute variance image
   ksize = 8;
   k = strel('disk',ksize);
   J = stdfilt(bgsub,k.Neighborhood).^2;

   % Threshold variance image
   thresh = 0.5e6;
   mask = J > thresh;

   % Erode mask
   ksize = 6;
   k = strel('disk',ksize);
   mask = imerode(mask,k);

   % Compute fractional coverage
   coverage = mean(mask(:));
```

Cell streaming was monitored over 62 hours on an Incucyte. Cell streaming anisotropy was quantified to measure directionality-dependent coordinated cell movement using FibrilTool (*43*). In ImageJ, images were segmented into 9 equal areas, and FibrilTool plugin was applied to each area. Anisotropy values were then averaged in Excel. Stream width was quantified manually on ImageJ 62 hours after seeding of KPC cells on CDMs.

Fluid shear stress assay. KPC cells were cultured +/- Fasudil (5 μM) for 72 hours before being subjected to fluid shear stress, as previously performed (*106*). Briefly, cells were trypsinized and resuspended to a concentration of $5x10^5$ cells/ml of culture medium. An aliquot was isolated and used as a "P0" sample, not subjected to shear stress. A second aliquot was subjected to five repeated exposures to shear stress ("P5" sample) through a 30-gauge needle, and a constant flow of 100 μl/sec was applied. Poiseuille's equation was used to measure shear stress: $\tau = 4Q\eta/\pi R^3$, where Q is flow rate in (0.1 cm^3/s), η is the

dynamic fluid viscosity of the medium (culture medium at room temperature; $0.78x10^{-3}$ N.s/m^2), and R is the needle radius ($R=7.95\times10^{-3}$ cm). τ_{max}=1950 dyn/cm^2, which is in the range of shear stress found in physiological conditions (*106*).

After shear stress, $2x10^4$ KPC cells were seeded on CDMs (12-well plate), and cell attachment was followed over 24 hours. Cell death on CDMs after shear stress was also assessed by cleaved caspase-3 staining 48 hours after shear stress. KPC cells were also seeded on plastic ($1x10^6$ cell/T75 flask), and cell proliferation was assessed using a Cell Counter. Cell death 24 hours after shear stress was assessed by FACS using the annexin V (FITC)/propidium iodide (PI) staining kit (Biovision) as per the manufacturer's instructions. Flow cytometry was performed using FACS Canto II (Becton Dickinson) and analyzed using the FlowJo software (Tree Star Inc.).

Anchorage-independent growth (AIG) assay. AIG assays were performed as previously described (*95*). Briefly, 1% agarose (Quantum Scientific) was first added to 12-well plates and allowed to solidify at room temperature for 1 hour. KPC cells were trypsinized and filtered to obtain a single cell suspension. Subsequently, KPC cells were suspended in a 0.3% agarose solution (2,000 cells/ml) and plated over the 1% cell-free agarose layer. The mixture of cells and agarose was allowed to solidify at 37^0C for 30 min, and samples were imaged to validate the absence of cell clusters and treated +/- Fasudil (5 μM). After 7 days of growth in the presence or absence of Fasudil, samples were treated +/- gemcitabine (100 nM)/Abraxane (100 nM) for 72 hours. Cell clusters were then imaged on a DM4000 Leica microscope, and cluster size was measured in ImageJ.

Quantification of mitotic defects in subcutaneous KPC xenografts. Mitotic defects were quantified on H&E stained sections of KPC xenografts. Quantification was based on nuclear shape, DNA condensation, and position in the cell. Cells in prophase and metaphase were classified as "early mitotic" cells, whereas cells in anaphase, telophase, and cytokinesis were classified as "late mitotic" cells. 10 images per tumor were quantified.

PC arrays from the Australian Pancreatic Cancer Genome Initiative (APGI) cohort. A cohort of 104 patients with primary operable, untreated PC who underwent pancreatectomy with curative intent (preoperative clinical stages I and II) was recruited as part of the APGI and the International Cancer Genome Consortium. Detailed clinical and pathologic characteristics of the cohort have been previously described (*18, 55*).

Automated SHG imaging of the ICGC TMA cohort. Widefield autofluorescence overview images of unstained TMA slides were produced by tiling multiple images acquired using a Leica DM6000 microscope with an automated stage using a 10x objective. The centroid of each core on the tiled image was manually marked in ImageJ and exported to a 'Mark and Find' file for the multi-photon microscope, correcting for the different relative coordinates of the microscope stage. Using the multi-photon microscope described previously, a 3D z-stack (30 μm depth with a z-step size of 2.5 μm) was automatically acquired for each core using a 20x objective. The sample was excited at 880 nm, and SHG and autofluorescence images were acquired using 440/20 and 490/40 emission filters, respectively. To correct for variations in the z-position of the sample, the focus point was corrected every four cores by imaging a 15 slice z-stack with 300 μm depth and setting the stack center to the z-position of the brightest slice.

Whole body IVIS spectrum imaging. Luciferase signal was imaged as a readout of orthotopic tumor growth and spread on an IVIS Spectrum. Luciferin (150 mg/kg, Gold Biotechnology) was administered by intraperitoneal injection. Mice were anaesthetized (isoflurane 3 L, O_2 1 L/min, vacuum was used constantly to remove excess of O_2) and placed on the IVIS stage with the left flank exposed. Signal was acquired with open filters and small binning. Total flux was determined as a measure of tumor burden.

Immunohistochemistry staining. Tissues were fixed in 10% buffered formalin and embedded in paraffin. 4 μm sections were placed in xylene for de-paraffinization and rehydrated using graded ethanol washes. Antigen retrieval was performed using target retrieval solution low-pH (S1699) for 30 min in a water bath (93ºC for organotypic samples and 100ºC for mouse tissues). For immunohistochemistry staining, slides were quenched in 3% H_2O_2 before application of protein block (Dako). The slides were incubated with primary antibodies (table S2, and secondary antibodies (Envision) coupled to HRP were applied. Detection was achieved with diaminobenzidine (DAB). H&E staining and counterstaining were performed on a Leica autostainer.

Analysis of mTurquoise2 lifetime in organotypic matrices. FLIM data from the SRC biosensor in organotypic matrices were analyzed using FLIMfit (*107*) by fitting to a single exponential lifetime model using a Maximum Likelihood estimator accounting for the instrument response function and contribution for incomplete decays. A 3 x 3 spatial smoothing kernel was applied. Average lifetime values per cell were calculated using masks created by manually segmenting the intensity images.

Quantification of picrosirius red staining image with non-polarized light. The area covered by collagen I and III was quantified in ImageJ software (US National Institutes of Health) using an in-house script (see below)

```
//Picrosirius analysis//
requires("1.44l");
num = nImages;
lower = 0; upper = 0;
dir1 = getDirectory("Choose a Directory ");
dir2 = dir1;
OpenFiles1(dir1,dir2);
function OpenFiles1(dir1,dir2) {
	list = getFileList(dir1);
	for (i=0; i<list.length; i++) {
		if (endsWith(list[i], "/")){
			OpenFiles1(""+dir1+list[i],dir2);
		}
		else{
			if(endsWith(dir1+list[i], ".tif")==1){
				open(dir1+list[i]);
					run("Set Measurements...", "area mean limit display redirect=None decimal=3");
waitForUser("Set the scale and click global");	run("Set Scale...");
		run("HSB Stack");
	waitForUser("Please go to the Saturation window");
		waitForUser("Please set threshold");
		getThreshold(lower, upper);
		print(lower,upper);
	close();
		OpenFiles2(dir2,lower,upper);
run("Threshold...");
exit(); } } } }

function OpenFiles2(dir2,lower,upper) {
	list = getFileList(dir2);
	for (i=0; i<list.length; i++) {
		setBatchMode(true);
			if (endsWith(list[i], "/")) {
				OpenFiles2(""+dir2+list[i],lower,upper); }

		else{
			if(endsWith(dir2+list[i], ".tif")==1){
				open(dir2+list[i]);
				print(dir2+list[i]);
run("HSB Stack");
setAutoThreshold("Default dark");
setThreshold(lower, upper);
setOption("BlackBackground", false);
run("Convert to Mask", "method=Default background=Dark");
run("Stack to Images");
selectWindow("Saturation");
run("Analyze Particles...", "size=0-Infinity circularity=0-0.4 show=Masks summarize slices");
close();
```

Quantification of total area stained with CD31 in KPC tumors and in liver tissue. The area covered by CD31 staining was quantified in ImageJ software (US National Institutes of Health) using an in-house script (see below).

```
//CD31 area analysis//
requires("1.44l");
num = nImages;
for (j = 0; j < num; j++){
	close();
}
```

```
lower = 0; upper = 0;
dir1 = getDirectory("Choose a Directory ");
dir2 = dir1;
OpenFiles1(dir1,dir2);
function OpenFiles1(dir1,dir2) {
list = getFileList(dir1);
for (i=0; i<list.length; i++) {
        if (endsWith(list[i], "/")){
                OpenFiles1(""+dir1+list[i],dir2);
                }
                else{
                        if(endsWith(dir1+list[i], ".jpg")==1){
                                open(dir1+list[i]);
run("Set Measurements...", "area mean limit display redirect=None decimal=3");
waitForUser("Set the scale and click global");     run("Set Scale...");
 run("RGB Stack");
waitForUser("Please go to the Blue window");
run("Threshold...");
waitForUser("Please set threshold");
getThreshold(lower, upper);
print(lower,upper);
close();
OpenFiles2(dir2,lower,upper);
exit();
                        }
                }
        }
}

function OpenFiles2(dir2,lower,upper) {
        list = getFileList(dir2);
for (i=0; i<list.length; i++) {
                setBatchMode(true);
                        if (endsWith(list[i], "/")) {
                                OpenFiles2(""+dir2+list[i],lower,upper);
                                }
                else{
                        if(endsWith(dir2+list[i], ".jpg")==1){
                                open(dir2+list[i]);
                                print(dir2+list[i]);

run("RGB Stack");
setAutoThreshold("Default dark");
setThreshold(lower, upper);
setOption("BlackBackground", false);
run("Convert to Mask", "method=Default background=Dark");
run("Stack to Images");
selectWindow("Blue");
run("Analyze Particles...", "size=0-Infinity circularity=0-0.4 show=Masks summarize slices");
close();
setBatchMode(false);
                        }
                }
        }
}

exit()
run("CD31 area analysis.txt");
```

Supplementary figure 1

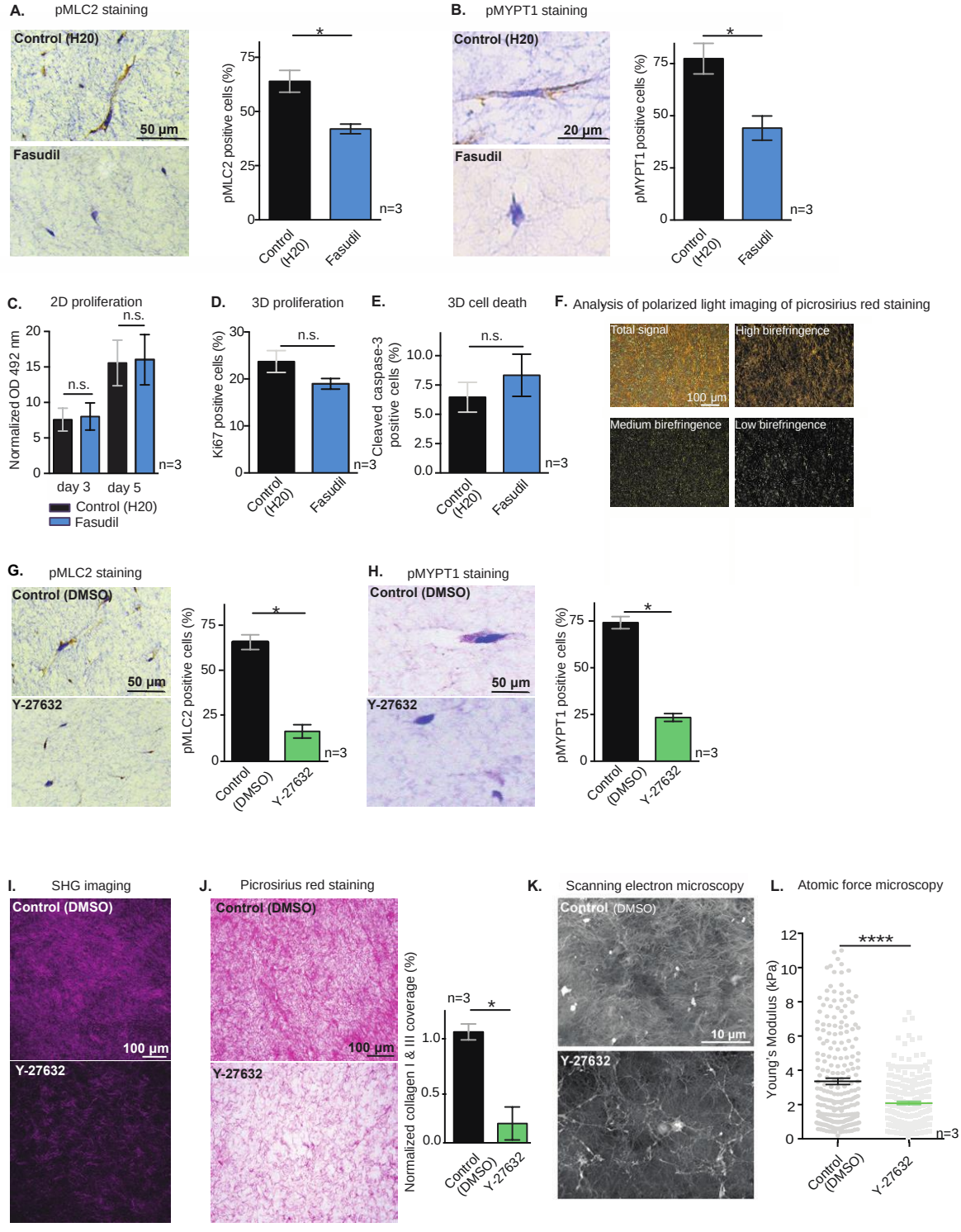

Fig. S1. ROCK inhibition with Fasudil and Y-27632 impairs ECM integrity. (**A**) IHC staining and quantification of pMLC2 and (**B**) pMYPT1 after a 12-day contraction assay +/- Fasudil. n=3 biological repeats with three matrices per condition and per repeat. (**C**) MTS analysis of telomerase immortalized fibroblast (TIFs) proliferation +/- Fasudil in 2D. n=3 biological repeats with three wells per condition and per repeat. (**D**) Quantification of TIFs proliferation in organotypic matrices via IHC staining with Ki67 after a 12-day contraction assay in presence or absence of Fasudil. n=3 biological repeats with three matrices per condition and per repeat. (**E**) Quantification of TIFs death in organotypic matrices via IHC staining for cleaved caspase-3 after a 12-day contraction assay in presence or absence of Fasudil. n=3 biological repeats with three matrices per condition and per repeat. (**F**) Representative images of signal emitted from collagen fibers with high (red/orange), medium (yellow), and low (green) birefringence in collagen matrices stained with picrosirius red and imaged with polarized light microscopy. (**G**) IHC staining and quantification of pMLC2 and (**H**) pMYPT1 after a 12-day contraction assay +/- Y-27632. n=3 biological repeats with three matrices per condition and per repeat. (**I**) Representative maximum intensity projections of SHG signal derived from organotypic matrices after a 12-day contraction assay +/- Y-27632. n=3 biological repeats with three matrices per condition and per repeat. (**J**) Representative images of picrosirius red staining imaged with non-polarized light and quantification of staining coverage in organotypic matrices after a 12-day contraction assay +/- Y-27632 (normalized to control). n=3 biological repeats with three matrices per condition and per repeat. (**K**) Representative scanning electron microscopy images of organotypic matrices after a 12-day contraction assay +/- Y-27632. (L) Atomic force microscopy analysis of collagen stiffness in organotypic matrices after a 12-day contraction assay in presence or absence of Y-27632. n=3 biological repeats with three matrices per condition and per repeat. Results are mean +/- SEM. p values were determined by unpaired, nonparametric t-test with a Mann-Whitney U correction.

Supplementary figure 2

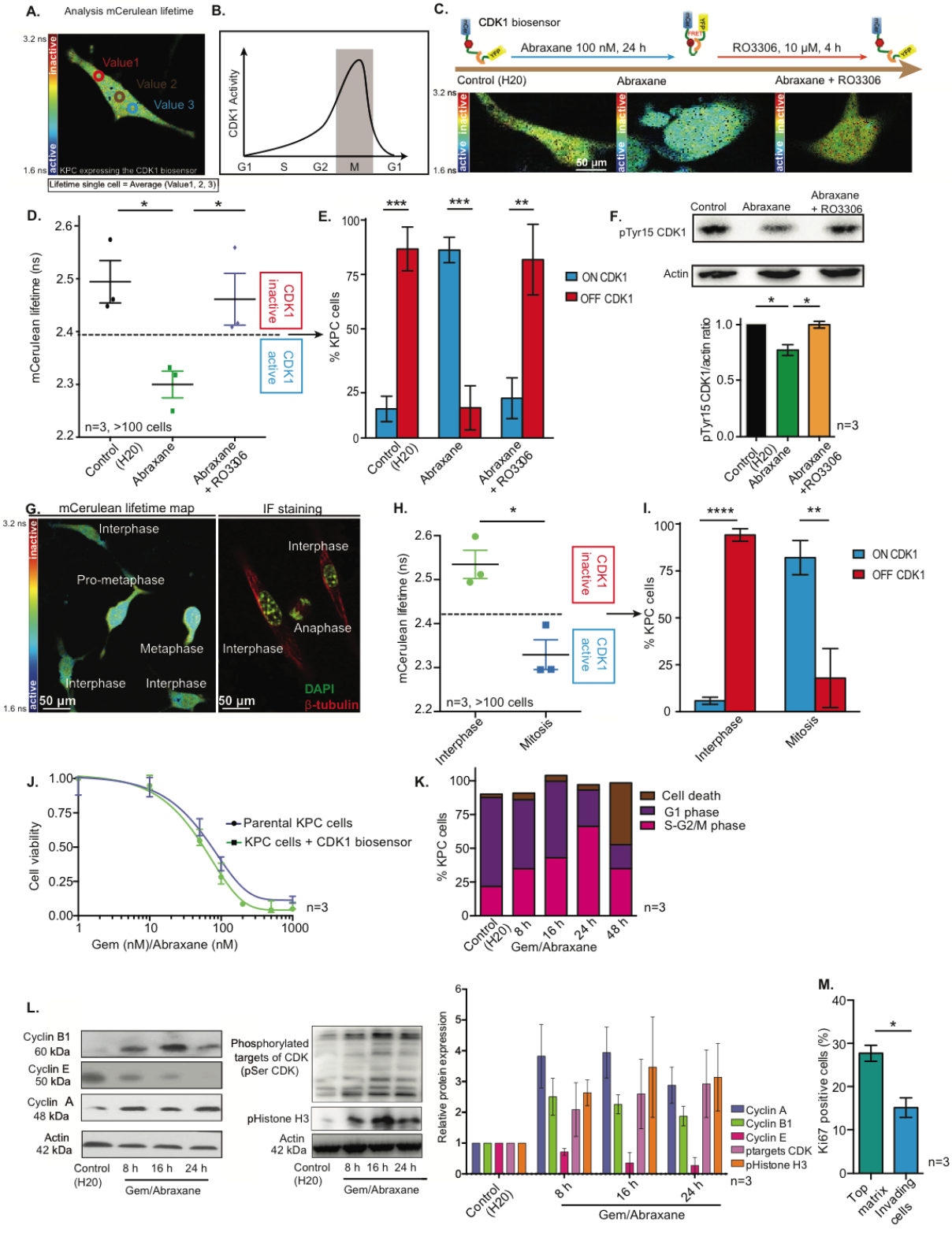

Fig. S2. The CDK1-FRET biosensor distinguishes changes in CDK1 activity and is a surrogate for cell cycle arrest. (**A**) Analysis of CDK1 activity in single cells is achieved by measuring mCerulean lifetime in 3 representative areas per cell to generate an average value. (**B**) Schematic representation of CDK1 activity during cell cycle. (**C**) Representative mCerulean lifetime maps, (**D**) quantification of mCerulean lifetimes, and (**E**) distribution of CDK1 activity in KPC cells upon treatment with Abraxane (24 hours, 100 μM) followed by treatment with the CDK1 inhibitor RO3306 (10 μM, 4 hours). (**F**) Western Blot analysis of pTyr15-CDK1 in response to treatment with Abraxane and with RO3306. (**G**) Representative mCerulean lifetime maps and β-tubulin immunofluorescence staining of KPC cells in mitosis and interphase. (**H**) Quantification of mCerulean lifetimes and (**I**) stratification of CDK1 activation in KPC cells in mitosis and interphase. n=3 independent biological repeats. (**J**) MTS analysis of cell viability upon treatment with Gem/Abraxane in primary KPC cells and KPC cells expressing the CDK1-FRET biosensor. n=3 independent biological repeats with three wells/condition. (**K**) DNA FACS analysis and (**L**) Western Blot analysis of KPC progressive cell cycle arrest and activation of CDK1 upon treatment with Gem/Abraxane. (**M**) Quantification of cell proliferation for KPC cells on top of collagen matrix or invading through the matrix. n=3 independent biological repeats with three technical replicates per repeat and per condition. Results are mean +/- SEM, unless stated otherwise, n=3 independent biological repeats with 1 technical replicate per repeat and treatment group. p values were determined by unpaired, nonparametric t-test with a Mann-Whitney U.

Supplementary figure 3

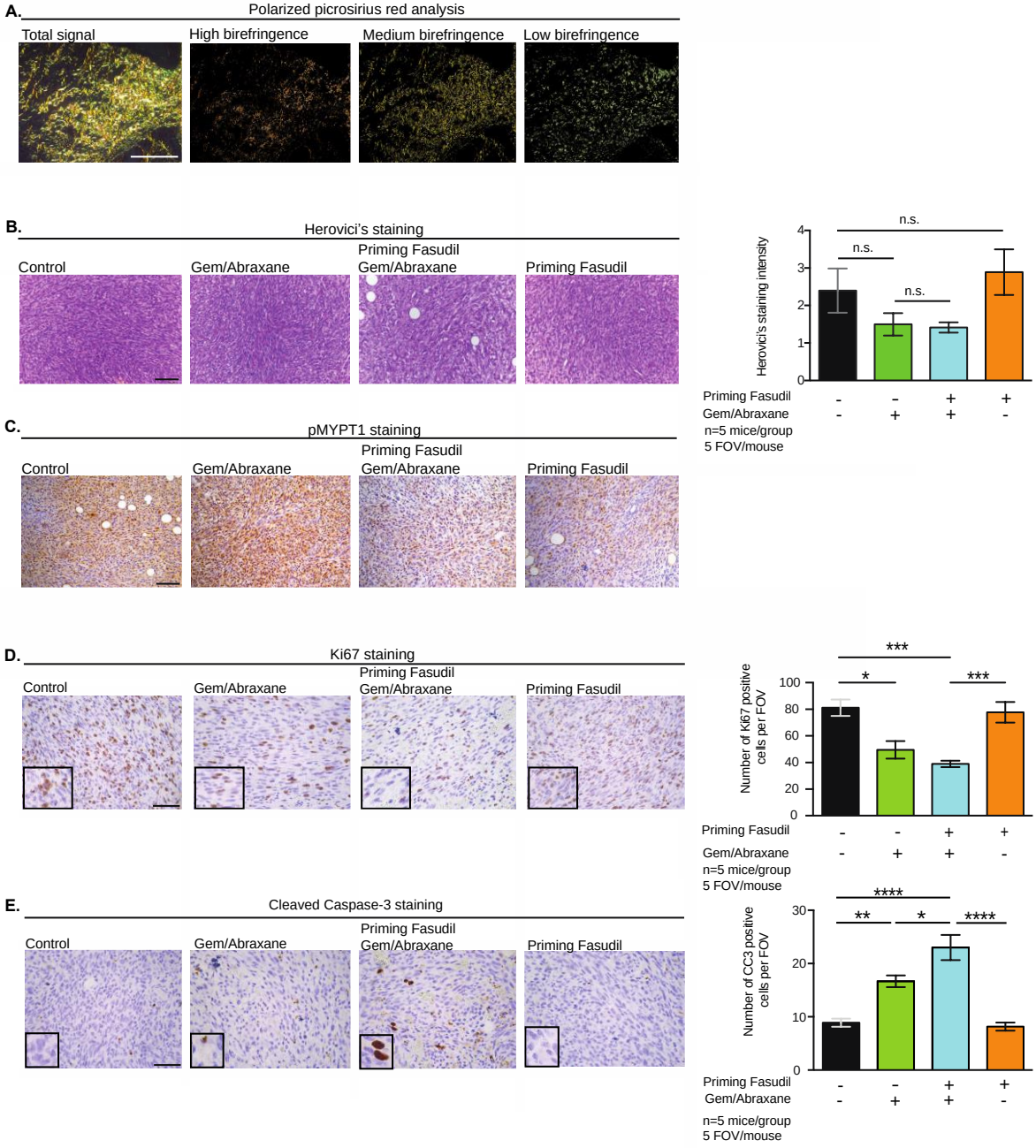

Fig. S3. Priming with Fasudil disrupts ECM remodeling, inhibits ROCK signaling, and improves Gem/Abraxane efficacy in vivo. (**A**) Representative images of signal emitted from collagen fibers with high (red/orange), medium (yellow), and low (green) birefringence in subcutaneous KPC tumors stained with picrosirius red and imaged with polarized light microscopy. n=5 mice/group, 5 FOV/mouse. (**B**) Herovici's staining of subcutaneous KPC tumors and quantification of collagen content upon treatment with control (saline); Gem/Abraxane; Fasudil then Gem/Abraxane; and Fasudil alone. n=5 mice/group, 5 FOV/mouse. (**C**) Representative images of pMYPT1 staining of KPC subcutaneous xenografts upon treatment with control (saline); Gem/Abraxane; Fasudil then Gem/Abraxane; and Fasudil alone. n=5 mice/group. (**D**) Ki67 staining and quantification in KPC subcutaneous xenografts upon treatment with control (saline); Gem/Abraxane; Fasudil then Gem/Abraxane; and Fasudil alone. n=5 mice/group, 5 FOV/mouse. Boxes are higher magnifications of portion of images, to highlight positive and negative staining. (**E**) Cleaved caspase-3 staining and quantification in KPC subcutaneous xenografts upon treatment with control (saline); Gem/Abraxane; Fasudil then Gem/Abraxane; and Fasudil alone. Boxes are higher magnifications of portion of images, to highlight positive and negative staining. n=5 mice/group, 5 FOV/mouse. Results are mean +/- SEM. Scale bars= 50 μm. p values were determined by nonparametric ANOVA test with a Holm-Sidak correction for multiple comparison.

Supplementary figure 4

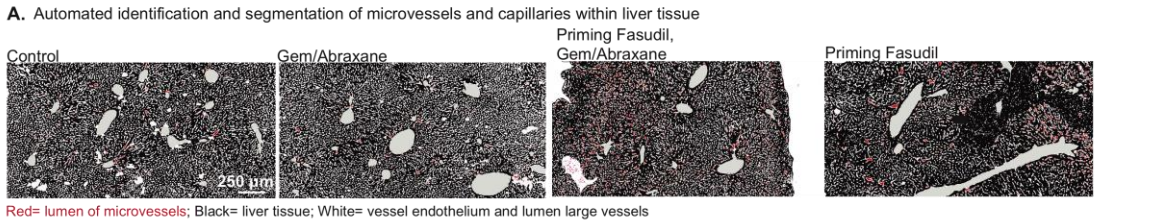

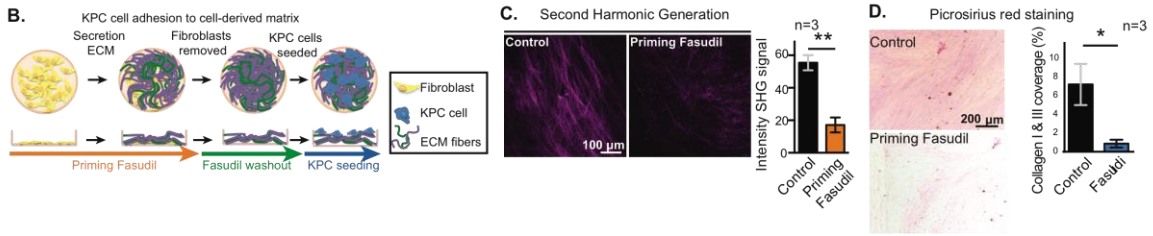

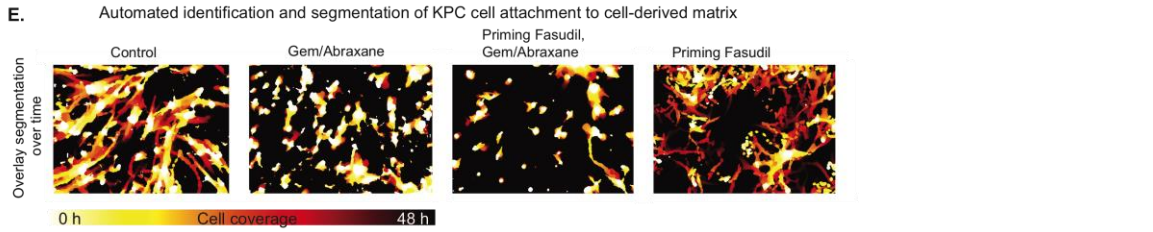

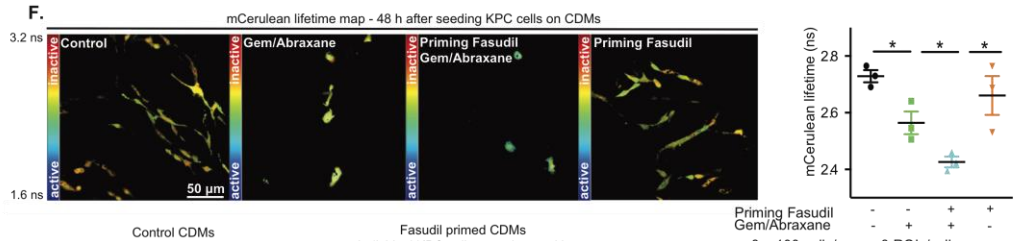

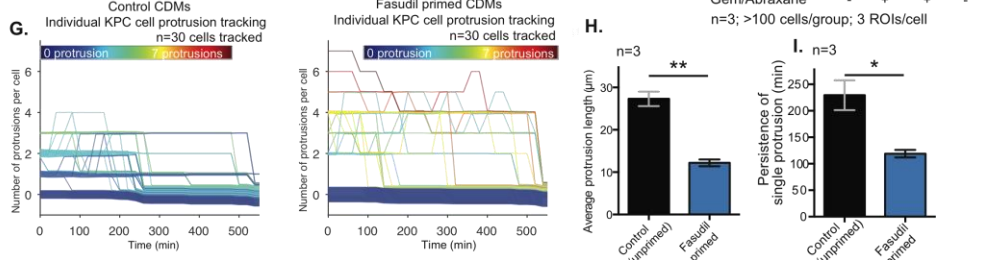

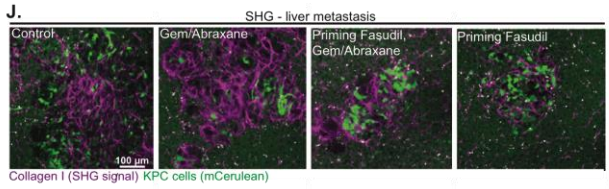

Fig. S4. Priming with Fasudil influences liver vasculature, cell attachment to CDMs, response to chemotherapy, and remodeling of the ECM. (**A**) Automated identification of microvessel and capillary lumens and representative images of segmentation performed on Amira 6 in liver tissue upon treatment with control (saline); Gem/Abraxane; Fasudil then Gem/Abraxane; and Fasudil alone. Capillary lumen is highlighted in red, whereas the rest of the tissues segmented are represented in different shades of gray. (**B**) Schematic representation of cell-derived matrix establishment followed by KPC cell attachment. (**C**) Maximum intensity projection and quantification of SHG signal from CDMs unprimed or primed with Fasudil. (**D**) Picrosirius red staining and quantification of CDMs unprimed and primed with Fasudil. (**E**) Automated identification and quantification of KPC cells attaching on CDMs unprimed or primed with Fasudil and/or treated with Gem/Abraxane. (**F**) Representative mCerulean lifetime maps and quantification of mCerulean lifetime in KPC cells expressing the CDK1 biosensor, seeded on CDMs unprimed or primed with Fasudil +/- Gem/Abraxane for 48 hours. Results are mean +/- SEM, n=3 repeats, 100 cells/group, 3 ROIs/cell. (**G**) Tracking of number of protrusions per KPC cell over time. Traces are color coded according to the initial number of protrusions (at t=0 min). (**H**) Quantification of single KPC cell protrusion average length and (**I**) persistence on CDMs unprimed or primed with Fasudil. n=3 repeats, 30 cells per conditions were tracked. (**J**) Representative images of live SHG imaging (magenta) in KPC metastases (mCerulean fluorescence, green) in freshly harvested liver tissue. p values were determined by unpaired, nonparametric t-test with a Mann-Whitney U correction (comparison between two groups), nonparametric ANOVA test with a Holm-Sidak correction for multiple comparison (more than two groups).

Supplementary figure 5

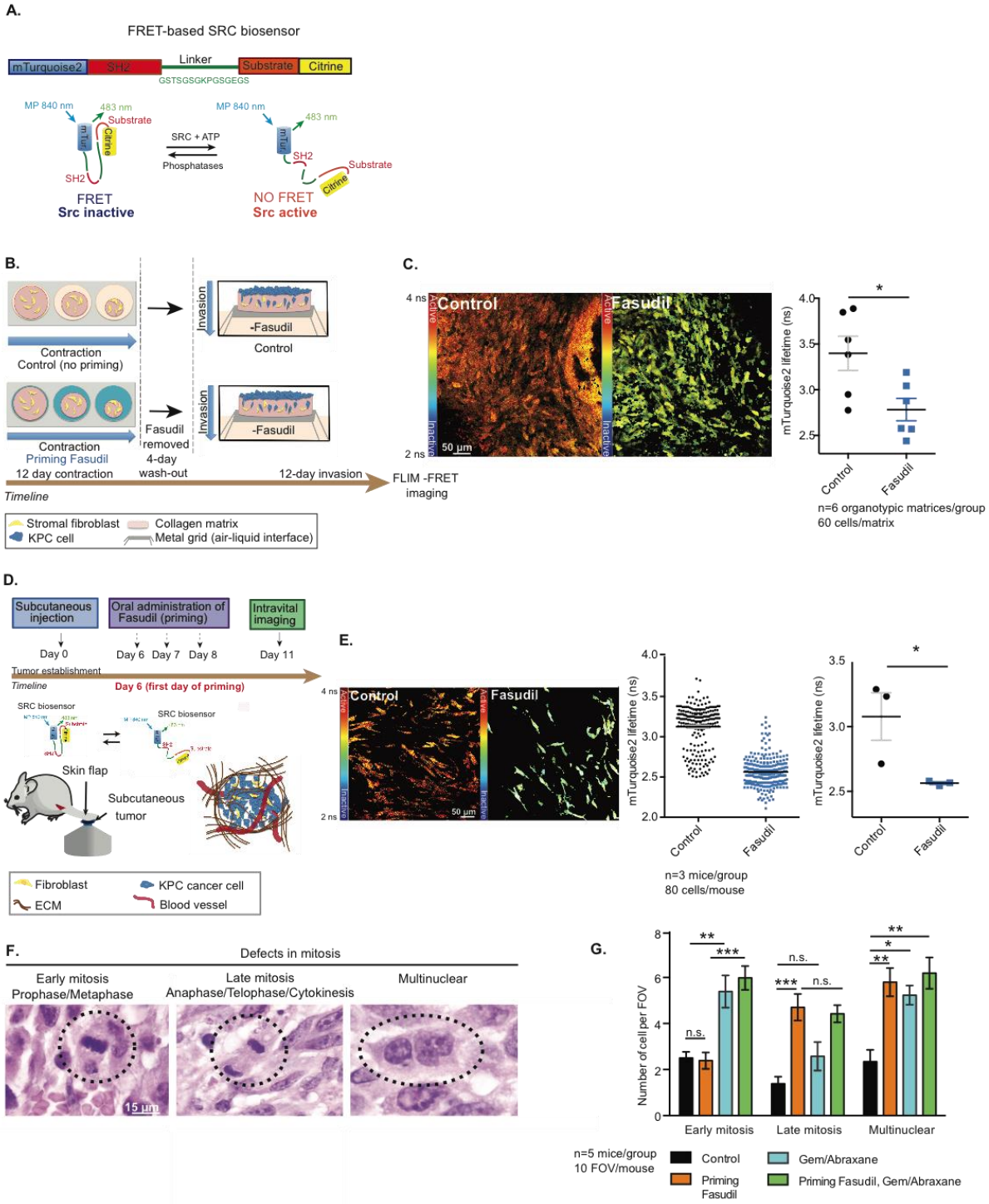

Fig. S5. Priming with Fasudil results in decreased SRC activity and defects in mitosis. (**A**) Schematic representation of the FRET-based SRC biosensor. (**B**) Schematic representation of organotypic invasion assay. (**C**) FLIM-FRET imaging of the SRC biosensor in KPC cells invading through organotypic matrices unprimed or primed with Fasudil. n=6 organotypic matrices from 2 independent biological repeats, 60 cells/matrix. (**D**) Schematic representation and (**E**) intravital FLIM-FRET imaging and quantification of SRC activity in subcutaneous KPC tumors unprimed or primed with Fasudil. n=3 mice/group, 80 cells/mouse. (**F**) Representative images and (**G**) quantification of mitotic defects in subcutaneous KPC tumors upon treatment with control (saline); Gem/Abraxane; Fasudil then Gem/Abraxane; or Fasudil alone. n=5 mice/group, 10 FOV/mouse. p values were determined by unpaired, nonparametric t-test with a Mann-Whitney U correction (comparison between two groups), nonparametric ANOVA test with a Holm-Sidak correction for multiple comparison (more than two groups).

Supplementary figure 6

TKCC5 'high' ECM PDX model

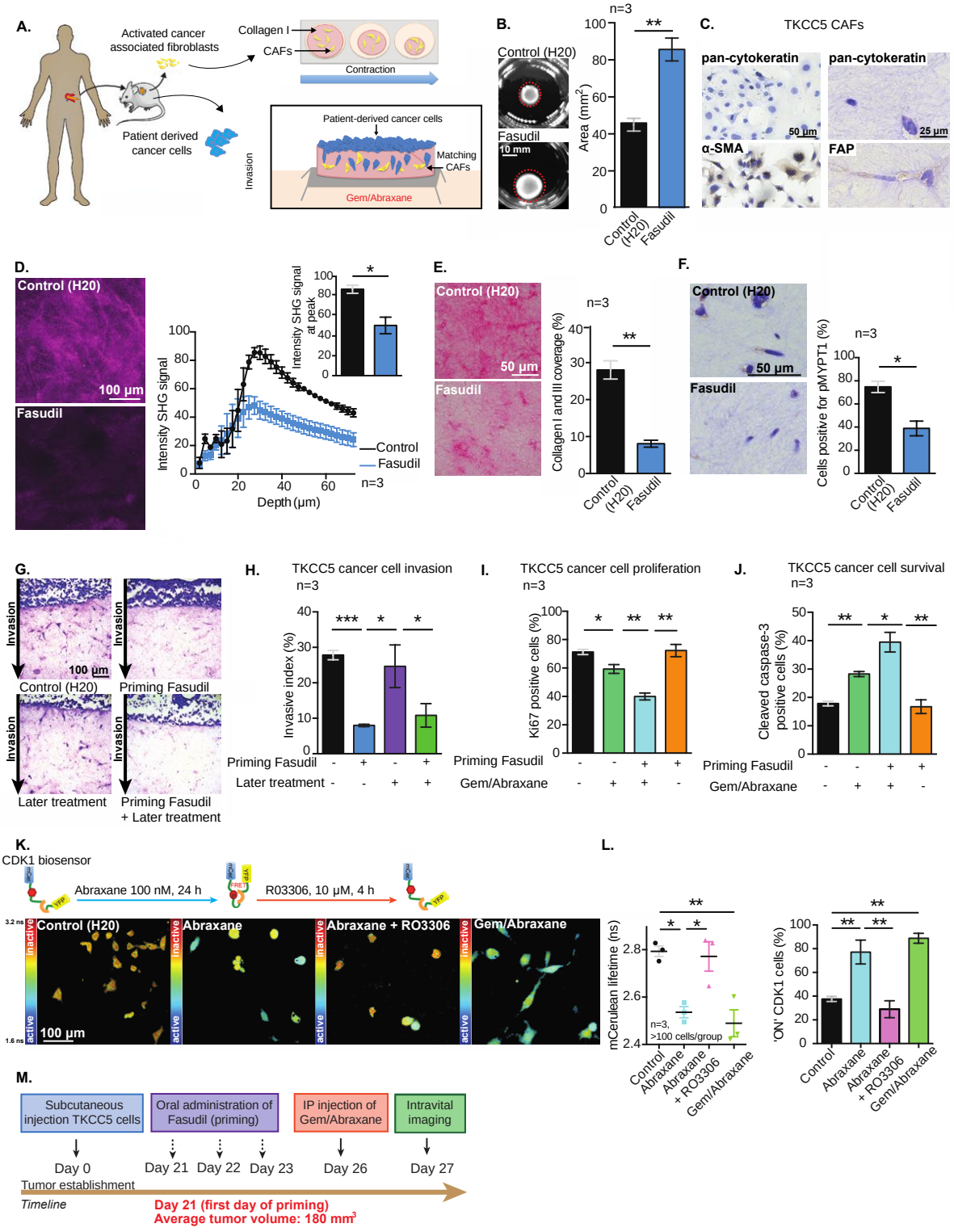

Fig. S6. High ECM TKCC5 patient model responds to priming strategies in a 3D patient-personalized organotypic matrix. (**A**) Schematic representation of isolation of patient-derived cancer cells and activated CAFs from TKCC5 PDX tumors. Matched cancer cells and CAFs were used to generate patient-personalized organotypic matrices. TKCC5 CAFs were embedded in collagen and allowed to contract for 7 days before seeding of TKCC5 cancer cells and invasion. (**B**) Representative images of TKCC5 CAFs-collagen matrices and quantification of matrix area after a 7-day contraction assay +/- Fasudil. n=3 biological repeats with three matrices per condition and per repeat. (**C**) IHC characterization of TKCC5 CAF in 2D settings (left panel) and 3D collagen matrix (right panel). Pancytokeratin staining marks epithelial cells, whereas activated fibroblasts are positive for FAP and α-SMA. (**D**) Representative maximum intensity projections of SHG imaging and quantification of SHG signal intensity by depth (line curve) and at peak (histogram inset) in TKCC5 CAFs-collagen matrices after a 7-day contraction assay +/- Fasudil. n=3 biological repeats with three matrices per condition and per repeat. (**E**) Representative images and quantification of picrosirius red staining imaged by non-polarized light microscopy and (**F**) pMYPT1 staining of TKCC5 CAFs-collagen matrices after a 7-day contraction assay +/- Fasudil. n=3 biological repeats with three matrices per condition and per repeat. (**G**) H&E staining of TKCC5-patient personalized organotypic matrices and (**H**) quantification of TKCC5 cancer cell invasive index in matrices primed with Fasudil during contraction and/or treated with Fasudil during invasion. n=3 biological repeats with three matrices per condition and per repeat. (**I**) Quantification of TKCC5 cancer cell proliferation (Ki67 staining) and (**J**) apoptosis (cleaved caspase-3 staining) upon priming with control or Fasudil and subsequent treatment with Gem/Abraxane in patient-personalized organotypic matrices. n=3 biological repeats with three matrices per condition and per repeat. (**K**) Representative mCerulean lifetime maps and (**L**) quantification of mCerulean lifetime and of CDK1 activity in TKCC5 cancer cells expressing the CDK1 biosensor and upon treatment with control; Abraxane alone; Abraxane followed by treatment with RO3306; or Gem/Abraxane. n=3 independent biological repeats, >100 cells/group, 3 ROIs/cell. (**M**) Schematic representation of subcutaneous injection of TKCC5 cells and treatment timeline. Priming of TKCC5 tumors started on day 21 after injection, when tumors were established (average tumor volume: 180 mm^3). Results are mean +/- SEM, p values were determined by unpaired, nonparametric t-test with a Mann-Whitney U correction (comparison between two groups), nonparametric ANOVA test with a Holm-Sidak correction for multiple comparison (more than two groups).

Supplementary figure 7

TKCC2 'low ECM' PDX model

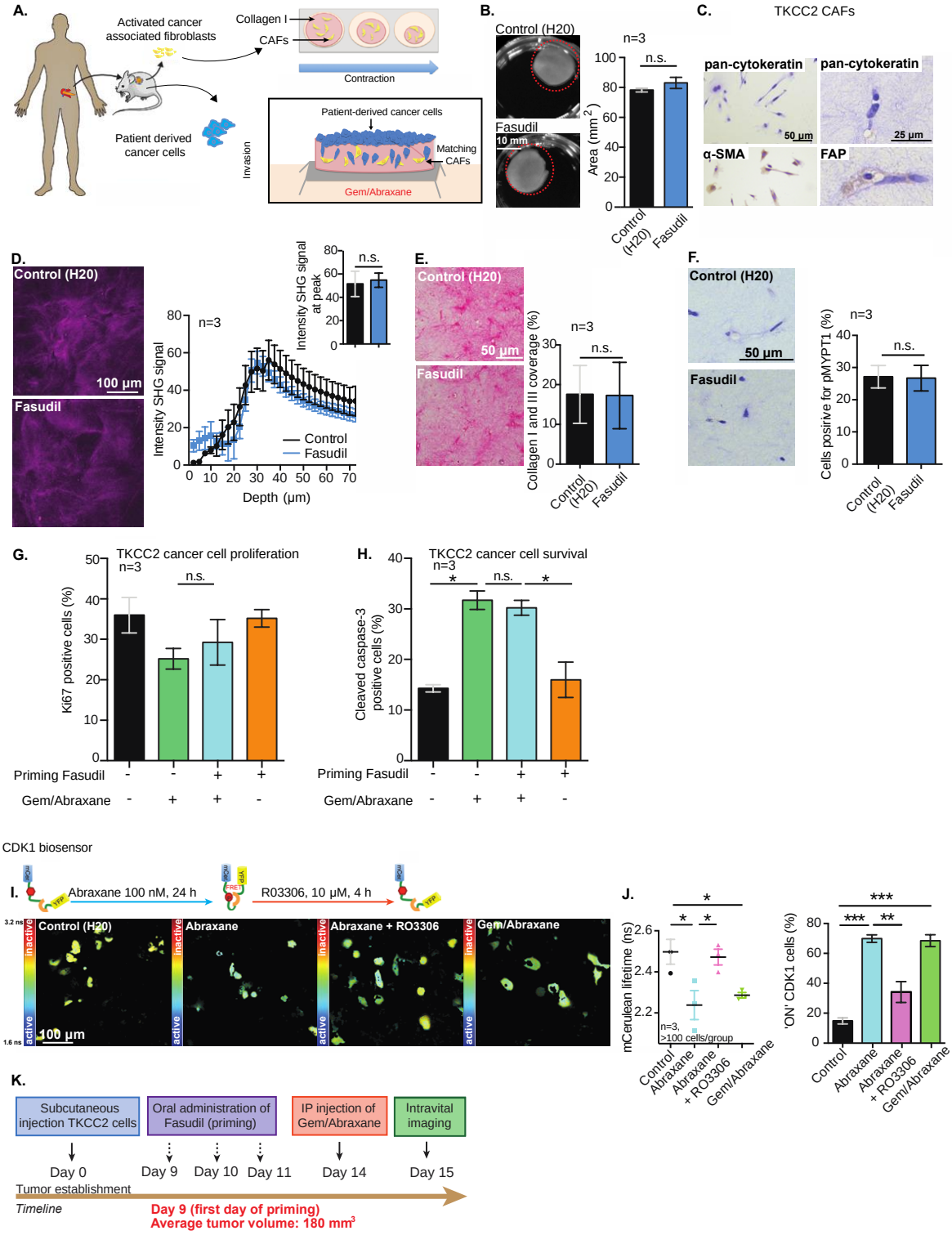

Fig. S7. Low ECM TKCC2 patient model does not respond to priming strategies in a 3D patient-personalized organotypic matrix. (**A**) Schematic representation of isolation of patient-derived cancer cells and activated CAFs from TKCC2 PDX tumors. Matched cancer cells and CAFs were used to generate patient-personalized organotypic matrices. TKCC2 CAFs were embedded in collagen and allowed to contract for 7 days before seeding of TKCC2 cancer cells and invasion. (**B**) Representative images of TKCC2 CAFs-collagen matrices and quantification of matrix area after a 7-day contraction assay +/- Fasudil. n=3 biological repeats with three matrices per condition and per repeat. (**C**) IHC characterization of TKCC2 CAF in 2D settings (left panel) and 3D collagen matrix (right panel). Pancytokeratin staining marks epithelial cells, whereas activated fibroblasts are positive for FAP and α-SMA. (**D**) Representative maximum intensity projections of SHG imaging and quantification of SHG signal intensity by depth (line curve) and at peak (histogram inset) in TKCC2 CAFs-collagen matrices after a 7-day contraction assay +/- Fasudil. n=3 biological repeats with three matrices per condition and per repeat. (**E**) Representative images and quantification of picrosirius red staining imaged by non-polarized light microscopy and (**F**) pMYPT1 staining of TKCC2 CAFs-collagen matrices after a 7-day contraction assay +/- Fasudil. n=3 biological repeats with three matrices per condition and per repeat. (**G**) Quantification of TKCC2 cancer cell proliferation (Ki67 staining) and (**H**) apoptosis (cleaved caspase-3 staining) upon priming with control or Fasudil and subsequent treatment with Gem/Abraxane in patient-personalized organotypic matrices. n=3 biological repeats with three matrices per condition and per repeat. (**I**) Representative mCerulean lifetime maps and (**J**) quantification of mCerulean lifetime and of CDK1 activity in TKCC2 cancer cells expressing the CDK1 biosensor and upon treatment with control; Abraxane alone; Abraxane followed by treatment with R03306; or Gem/Abraxane. n=3 independent biological repeats. >100 cells/group, 3 ROIs/cell. (K) Schematic representation of subcutaneous injection of TKCC2 cells and treatment timeline. Priming of TKCC2 tumors started on day 9 after injection, when tumors were established (average tumor volume: 180 mm^3). Results are mean +/- SEM. p values were determined by unpaired, nonparametric t-test with a Mann-Whitney U correction (comparison between two groups), nonparametric ANOVA test with a Holm-Sidak correction for multiple comparison (more than two groups).

Supplementary figure 8

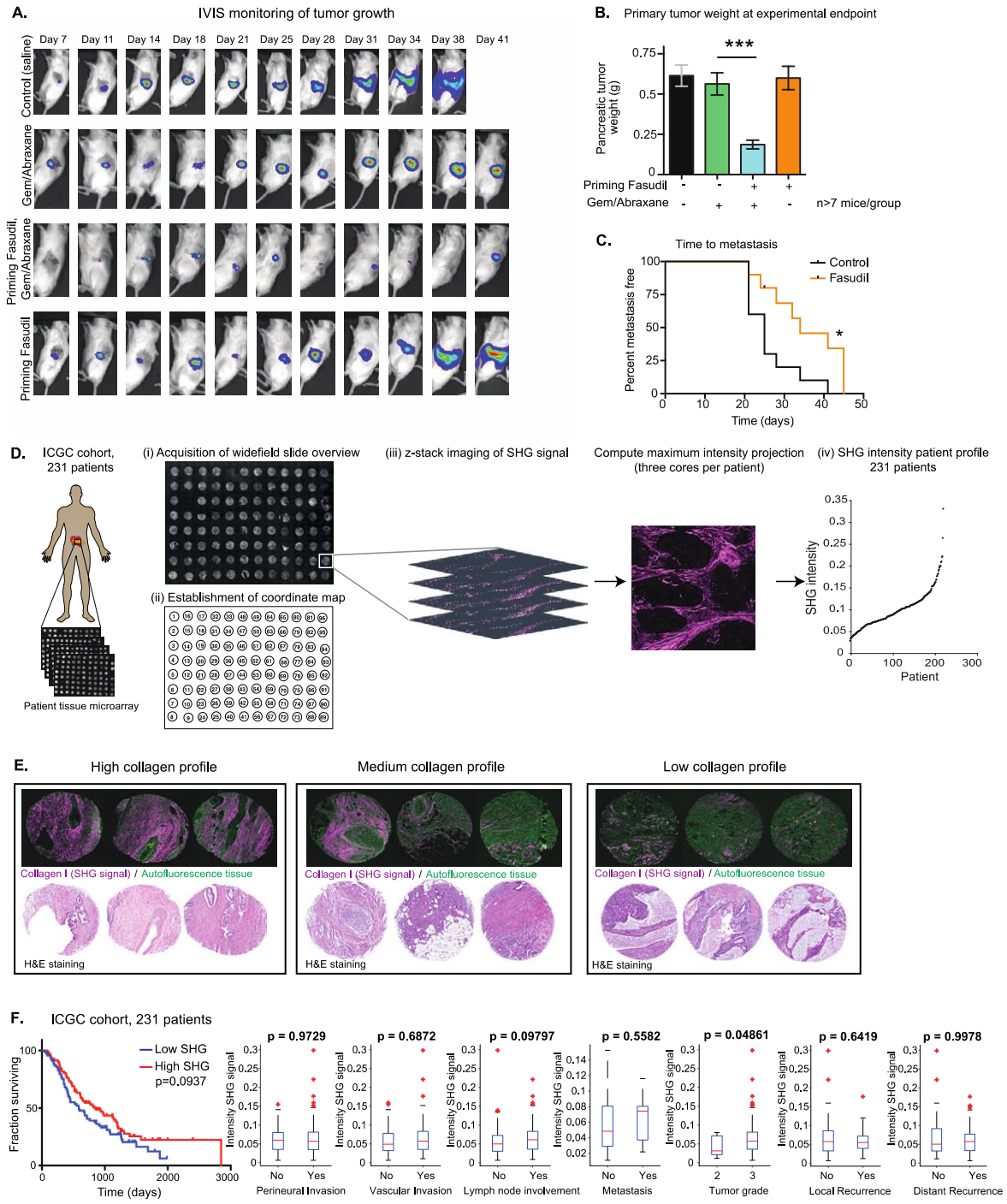

Fig. S8. TKCC5 orthotopic tumors respond to priming, and SHG does not predict survival. (**A**) Whole-body imaging of mice bearing luciferase-TKCC5 tumors over time. Also see Fig. 8F for treatment timeline. (**B**) Examination of tumor burden at experimental endpoint (mean survival control: 39 days; Gem/Abraxane: 51 days; Fasudil then Gem/Abraxane: 75 days; Fasudil alone: 43 days). Control, n=10 mice; Fasudil priming, n=9 mice; Gem/Abraxane, n=9 mice; Fasudil then Gem/Abraxane, n=7 mice. (**C**) Percentage of metastasis-free mice upon treatment with control (saline) or Fasudil. Control, n=10 mice; Fasudil priming, n=9 mice. (**D**) Flow-chart diagram of in-house automatized SHG analysis of patient samples from the ICGC cohort. (i) Patient cores were imaged on a widefield microscope, and (ii) coordinate maps were established from slide overview. (iii) SHG z-stacks were acquired for each core using defined coordinates, and maximum intensity projections were computed to (iv) quantify SHG intensity profile for each patient. (D) SHG/autofluorescence maximum intensity projections with corresponding H&E staining of three cores from patients with high, medium, or low collagen profiles. SHG/autofluorescence images were acquired using automated SHG imaging set up described in (D). (**E**) Analysis of survival and clinico-pathological difference between patients with high SHG versus patients with low SHG in the ICGC cohort. Patients who died of surgical complications or whose deaths were non-cancer-related were excluded from the survival analysis. Kaplan-Meier curves were compared using a log-rank Mantel-Cox test. p-values for multi-variate analysis were calculated using non-parametric ANOVA.

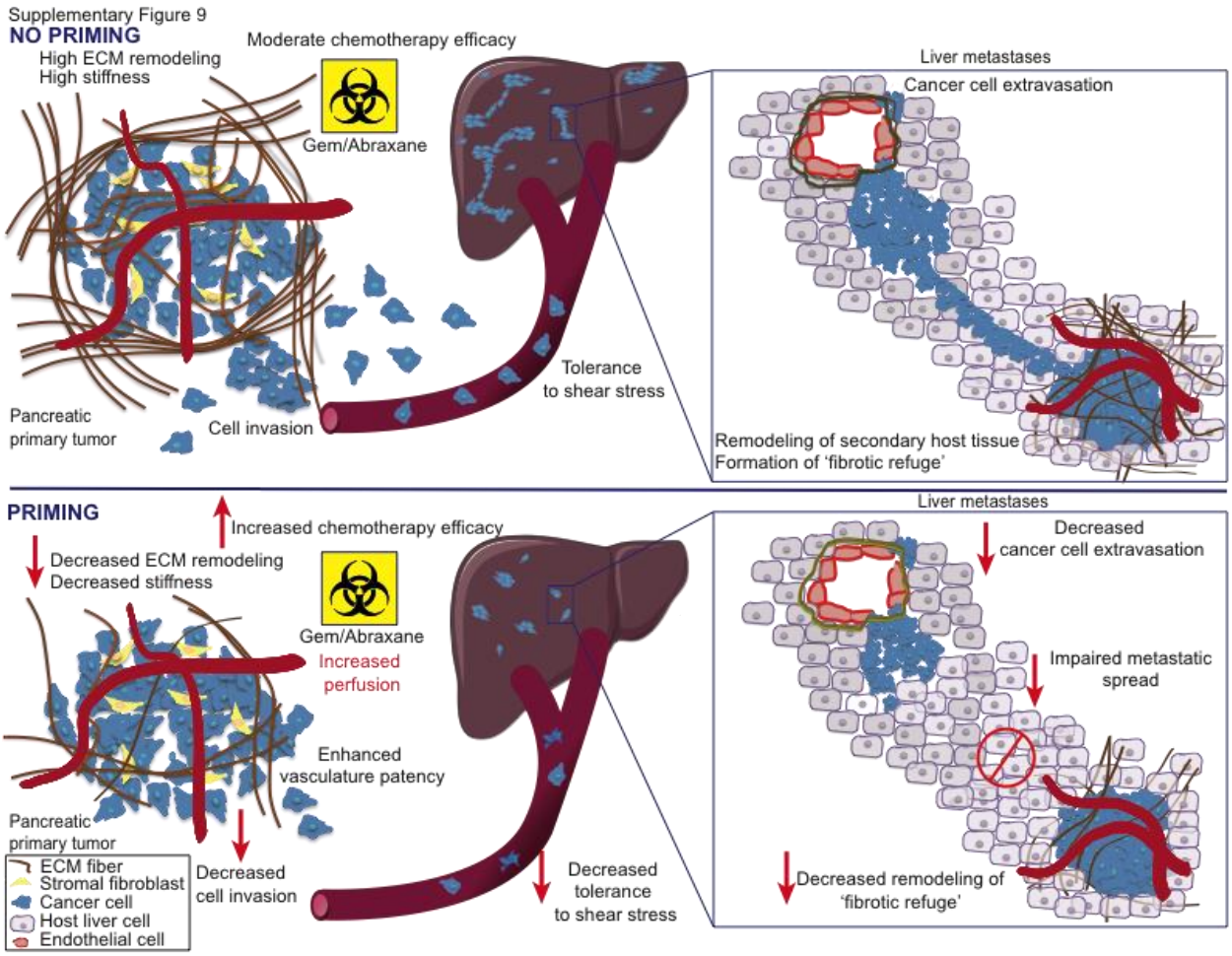

Fig. S9. Priming with Fasudil uncouples PC progression. Short-term manipulation of tumor tissue with Fasudil improves Gem/Abraxane efficacy in primary and secondary sites while rendering cancer cells more sensitive to shear stress and decreasing cell invasion, extravasation, and spread to secondary sites.

Table S1. List of *P* values.

Table S1 **List of p values**

Figure	Panel	Comparison and p value
Figure 1	Fig. 1B	Control vs Fasudil, p=0.0047
	Fig. 1C	Control vs Fasudil, p=0.0022
	Fig. 1D	High birefringence, control vs Fasudil, p=0.0125; medium birefringence, control vs Fasudil, p=0.0355; low birefringence, control vs Fasudil, p=0.0078
	Fig. 1E	Control vs Fasudil, p=0.9547
	Fig. 1F	Control vs Fasudil, p=0.4931
	Fig. 1H	Number of protrusions per cell, control vs Fasudil, p=0.0393; Average protrusion length, control vs Fasudil, p=0.0494; Persistence of single protrusion, control vs Fasudil, p=0.0244; Cell circularity, control vs Fasudil, p=0.0136
	Fig. 1J	Control vs Fasudil, p=0.0012
	Fig. 1K	Control vs Fasudil, p<0.0001
Figure 2	Fig. 2C	Control vs priming, p=0.019; control vs later treatment, p=0.9087; priming vs later treatment, p=0.0255; later treatment vs priming + later treatment, p=0.0218
	Fig. 2D	Control vs Gem/Abraxane, p=0.0466; Gem/Abraxane vs Fasudil, p=0.0062; Fasudil then Gem/Abraxane vs Fasudil alone: p=0.0106; control vs Fasudil, Gem/Abraxane, p=0.0037; control vs Fasudil, p=0.2432
	Fig. 2E	Control vs Gem/Abraxane, p=0.0466; Gem/Abraxane vs Fasudil then Gem/Abraxane, p=0.0028; Fasudil then Gem/Abraxane vs Fasudil alone, p=0.0091; control vs Fasudi then Gem/Abraxane, p=0.00987; control vs Fasudil, p=0.8711
Figure 3	Fig. 3B	mCerulean lifetimes, control vs Gem/Abraxane, p=0.0247; % KPC cells, control ON vs OFF, p=0.00479; Gem/Abraxane ON vs OFF, p=0.0071
	Fig. 3C	Comparisons CDK1 ON KPC cells, unprimed then Gem/Abraxane vs primed then Gem/ Abraxane -8 h: p=0.0036 -16 h: p=0.0022 -24 h: p=0.039 -48 h: p=0.0032
	Fig. 3D	Comparisons CDK1 ON KPC cells, unprimed then Gem/Abraxane vs primed then Gem/ Abraxane 48 h: p=0.0045

Figure	Panel	Comparison and p value
Figure 4	Fig. 4C	Control vs Fasudil, p=0.002; Gem/Abraxane vs Fasudil then Gem/Abraxane, p=0.0236; Control vs Fasudil then Gem/Abraxane, p=0.0014
	Fig. 4D	Total signal: Control vs priming Fasudil, p=0.0066; Gem/Abraxane vs Fasudil then Gem/Abraxane, p=0.0306 High birefringence: Control vs priming Fasudil, p=0.0442;Gem/Abraxane vs Fasudil then Gem/Abraxane, p=0.0487 Medium birefringence: Control vs priming Fasudil, p=0.0248;Gem/Abraxane vs Fasudil then Gem/Abraxane, p=0.0424 Low birefringence:Control vs priming Fasudil, p=0.0109
	Fig. 4E	mCerulean lifetimes: Control vs Gem/Abraxane, p=0.0435;Gem/Abraxane vs Fasudil then Gem/Abraxane, p=0.0473; Fasudil then Gem/Abraxane vs Fasudil alone, p=0.0061; Control vs Fasudil, p=0.6373 % cells with activated CDK1: Control vs Gem/Abraxane, p=0.0101;Gem/Abraxane vs Fasudil then Gem/Abraxane, p=0.0068; Fasudil then Gem/Abraxane vs Fasudil alone,p=0.0002; Control vs Fasudil, p=0.1318
	Fig. 4F	Control vs priming Fasudil, p=0.05; Gem/Abraxane vs Fasudil then Gem/Abraxane, p=0.0384
	Fig. 4H	Control vs priming Fasudil, p=0.0327
Figure 5	Fig. 5D	Control vs Gem/Abraxane, p=0.0193; Gem/Abraxane vs Fasudil then Gem/Abraxane, p=0.0471; Fasudil then Gem/Abraxane vs Fasudil, p=0.0022
	Fig. 5E	Control vs Gem/Abraxane, p=0.0485; Gem/Abraxane vs Fasudil then Gem/Abraxane, p=0.0431; Fasudil then Gem/Abraxane vs Fasudil, p=0.0008
	Fig. 5F	Area stained: Gem/Abraxane vs Fasudil then Gem/Abraxane, p=0.0078; Control vs Fasudil, p=0.0124 Number of microvessels: Control vs Fasudil, p=0.0481; Gem/Abraxane vs Fasudil then Gem/Abraxane, p=0.0181
	Fig. 5G	Control vs Gem/Abraxane, p=0.0313; Gem/Abraxane vs Fasudil then Gem/Abraxane, p=0.0249
	Fig. 5H	Control vs Gem/Abraxane, p=0.0357; Gem/Abraxane vs Fasudil then Gem/Abraxane, p=0.0462.

Figure	Panel	Comparison and p value
Figure 6	Fig. 6C	Control vs Fasudil priming, p=0.0005; Gem/Abraxane vs Fasudil then Gem/Abraxane, p=0.0003
	Fig. 6E	Control vs Fasudil-primed, p<0.0001; Gem/Abraxane vs Fasudil then Gem/Abraxane, p<0.0001
	Fig. 6G	Cell attachment onto CDMs, p=0.0487 Cell proliferation, p=0.0249 Apoptosis, p=0.05
	Fig. 6H	Annexin only, P5 control vs P5 Fasudil primed, p=0.0132 Annexin and PI, P5 control vs P5 Fasudil primed, p=0.0205
	Fig. 6J	Control vs Gem/Abraxane, p=0.0383; Control vs Fasudil, p=0.0471; Gem/Abraxane vs Fasudil then Gem/Abraxane, p=0.0421; Fasudil then Gem/Abraxane vs Fasudil, p=0.0107
Figure 7	Fig. 7B	Control vs priming Fasudil, p=0.0007
	Fig. 7C	Control vs priming Fasudil, p=0.0364
	Fig. 7D	Control vs priming Fasudil, p=0.0013; Gem/Abraxane vs Fasudil then Gem/Abraxane, p=0.0040
	Fig. 7G	Control no KPC cells vs Control with KPC cells, p=0.0453; Fasudil no KPC cells vs Fasudil with KPC cells, p=0.9492
	Fig. 7I	Control vs priming Fasudil, p=0.8475; Gem/Abraxane vs Fasudil then Gem/Abraxane, p=0.0874
	Fig. 7K	Control vs priming Fasudil, p=0.0103; Gem/Abraxane vs Fasudil then Gem/Abraxane, p=0.0062
Figure 8	Fig. 8B	TKCC2 vs TKCC5, p=0.0479
	Fig. 8C	High ECM TKCC5: Control vs priming Fasudil, p=0.0067; Gem/Abraxane vs Fasudil then Gem/Abraxane, p=0.0485 Low ECM TKCC2: Control vs priming Fasudil, p=0.7398; Gem/Abraxane vs Fasudil then Gem/Abraxane, p=0.9538
	Fig. 8D	High ECM TKCC5: Gem/Abraxane vs Fasudil then Gem/Abraxane, p=0.0019 Low ECM TKCC2: Gem/Abraxane vs Fasudil then Gem/Abraxane, p=0.0282
	Fig. 8E	TKCC2 priming Fasudil then Gem/Abraxane vs TKCC5 priming Fasudil then Gem/Abraxane, p=0.0479
	Fig. 8F	Kaplan Meier analysis, p=0.0006

Figure	Panel	Comparison and p value
figure S1	Fig. S1A	Control vs Fasudil, p=0.0371
	Fig. S1B	Control vs Fasudil, p=0.0.471
	Fig. S1C	Day 3 control vs Fasudil, p=0.8669; Day 5 control vs Fasudil, p=0.9281
	Fig. S1D	Control vs Fasudil, p=0.0748
	Fig. S1E	Control vs Fasudil, p=0.547
	Fig. S1G	Control vs Y-27632, p=0.0123
	Fig. S1H	Control vs Y-27632, p=0.0141
	Fig. S1J	Control vs Y-27632, p=0.0354
	Fig. S1L	Control vs Y-27632, p<0.0001
figure S2	Fig. S2D	Control vs Abraxane, p=0.0256; Abraxane vs Abraxane + RO3306, p=0.0273
	Fig. S2E	Control ON CDK1 vs OFF CDK1, p=0.0009; Abraxane ON CDK1 vs OFF CDK1, p=0.0009; Abraxane vs Abraxane + RO3306, p=0.0086
	Fig. S2F	Control vs Abraxane, p=0.0436; Abraxane vs Abraxane + RO3306, p=0.0436
	Fig. S2H	Interphase vs mitosis, p=0.0117
	Fig. S2I	Interphase ON CDK1 vs Interphase OFF CDK1, p<0.0001; Mitosis ON CDK1 vs mitosis OFF CDK1, p=0.0076
	Fig. S2M	Top matrix vs invading cells, p=0.0128
figure S3	Fig. S3B	Control vs Gem/Abraxane, p=0.4637; Gem/Abraxane vs Fasudil then Gem/Abraxane, p=0.8958; Control vs Fasudil, p=0.7016
	Fig. S3D	Control vs Gem/Abraxane, p=0.0226; Control vs Fasudil then Gem/Abraxane, p=0.0001; Fasudil then Gem/Abraxane vs Fasudil, p=0.0002
	Fig. S3E	Control vs Gem/Abraxane, p=0.0024; Gem/Abraxane vs Fasudil then Gem/Abraxane, p=0.0056; Fasudil then Gem/Abraxane vs Fasudil, p<0.0001; Control vs Fasudil then Gem/Abraxane, p<0.0001
figure S4	Fig. S4D	Control vs Fasudil priming, p=0.0476
	Fig. S4F	Control vs Gem/Abraxane, p=0.0492; Gem/Abraxane vs Fasudil then Gem/Abraxane, p=0.0495; Fasudil then Gem/Abraxane vs Fasudil, p=0.0131
	Fig. S4H	Control vs Fasudil, p=0.0013
	Fig. S4I	Control vs Fasudil, p=0.0191

Figure	Panel	Comparison and p value
figure S5	Fig. S5C	Control vs Fasudil, p=0.0481
	Fig. S5E	Control vs Fasudil (right hand panel), p=0.0425
	Fig. S5G	Early mitosis: Control vs Fasudil priming, p=0.8612; Control vs Gem/Abraxane, p=0.0020; Fasudil vs Fasudil then Gem/Abraxane, p=0.0003 Late mitosis: Control vs Fasudil, p=0.0008; Control vs Gem/Abraxane, p=0.1983; Fasudil vs Fasudil then Gem/Abraxane, p=0.6694 Multinuclear: Control vs Fasudil, p=0.0031; Control vs Gem/Abraxane, p=0.0158; Control vs Fasudil then Gem/Abraxane, p=0.0014
figure S6	Fig. S6B	Control vs Fasudil, p=0.0045
	Fig. S6D	Control vs Fasudil, p=0.0168
	Fig. S6E	Control vs Fasudil, p=0.0016
	Fig. S6F	Control vs Fasudil, p=0.0110
	Fig. S6H	Control vs priming Fasudil, p=0.0001; priming Fasudil vs later treatment Fasudil, p=0.0481; later treatment Fasudil vs priming + later treatment, p=0.05
	Fig. S6I	Control vs Gem/Abraxane, p=0.0283; Gem/Abraxane vs Fasudil then Gem/Abraxane, p=0.0079; Fasudil then Gem/Abraxane vs Fasudil, p=0.0028
	Fig. S6J	Control vs Gem/Abraxane, p=0.0010; Gem/Abraxane vs Fasudil then Gem/Abraxane, p=0.0342; Fasudil then Gem/Abraxane vs Fasudil, p=0.0056
	Fig. S6L	mCerulean lifetimes: Control vs Abraxane, p=0.0151; Abraxane vs Abraxane + RO3306, p=0.0183; Control vs Gem/Abraxane, p=0.0086 'ON' CDK1 cells: Control vs Abraxane, p=0.0084; Abraxane vs Abraxane + RO3306, p=0.0034; Control vs Gem/Abraxane, p=0.0029
Figure S7	Fig. S7B	Control vs Fasudil, p=0.2848
	Fig. S7D	Control vs Fasudil, p=0.8117
	Fig. S7E	Control vs Fasudil, p=0.9815
	Fig. S7F	Control vs Fasudil, p=0.9377
	Fig. S7G	Gem/Abraxane vs Fasudil then Gem/Abraxane, p=0.7549
	Fig. S7H	Control vs Gem/Abraxane, p=0.0266; Gem/Abraxane vs Fasudil then Gem/Abraxane, p=0.8488; Fasudil then Gem/Abraxane vs Fasudil, p=0.0306
	Fig. S7J	mCerulean lifetimes: Control vs Abraxane, p=0.0345; Abraxane vs Abraxane + RO3306, p=0.0415; Control vs Gem/Abraxane, p=0.05 'ON' CDK1 cells: Control vs Abraxane, p=0.0001; Abraxane vs Abraxane + RO3306, p=0.0016; Control vs Gem/Abraxane, p=0.0001

Figure	Panel	Comparison and p value
figure S8	Fig. S8B	Gem/Abraxane vs Fasudil then Gem/Abraxane, p=0.0009
	Fig. S8C	Control vs Fasudil, p=0.0209

Table S2. Details of antibodies used for the study.

Reagent/Antibody	Details	Dilution and references
Hematoxylin	Thermo Fisher Scientific # ASHB1000737AG	
Eosin Y solution	Sigma Aldrich #HT110332	
Herovici		as per online protocol http://stainsfile.info/StainsFile/stain/conektv/herovici.htm
Elastica Van Gieson		As per online protocol https://www.ihcworld.com/_protocols/special_stains/van_gieson_ellis.htm
Picrosirius red	Polysciences, #24901-250	as per commercial protocol
pMYPT1(Thr696)	Millipore #ABS45	1:100 (*6*)
Cleaved caspase-3	Cell Signaling #9661	1:100
Ki67	Thermo Scientific	1:500
CD31	Taylor Bio-Medical #DIA-310	1:120 for IHC, 1:100 for IF(*97*)
PDX-1	Abcam # 47267	1:1000
β-tubulin	Mouse Hybridoma	1:50
Tyr15CDK1	Cell Signaling #9111	1:500
Actin	Sigma Aldrich #A5441	1:1000
Cyclin E	Santa Cruz # M-20	1:500
Cyclin A	Santa Cruz # 596	1:500
Cyclin B	Cell Signaling # 4135	1:500
pMLC2 (Ser 19)	Cell Signaling #3671	1:200 (*6*)
pSer-CDK target	GeneSearch	1:1000
Pan-cytokeratin	Leica-Novostra C11	1:50
pHistone H3	GeneSearch	1:500
FAP	Abcam #53066	1:500 (*7*)
α-SMA	Abcam #5694	1:100

Movie S1. 4D monitoring of fibroblast-ECM interactions upon treatment with vehicle and Fasudil.
Fibroblasts: green, GFP
ECM: magenta, SHG
Related to Fig. 1.

Movie S2. Live FLIM-FRET imaging of the CDK1 biosensor in KPC cells in response to Abraxane and Abraxane + RO3306. *Related to Fig. S2.*

Movie S3. Live FLIM-FRET imaging of the CDK1 biosensor in KPC cells in interphase and mitosis. *Related to Fig. S2.*

Movie S4. Live FLIM-FRET monitoring of CDK1 activity in KPC cells actively interacting with an organotypic matrix. *Related to Fig. 3.*

Movie S5. Intravital FLIM-FRET imaging of subcutaneous xenografts with KPC-CDK1 cells and imaging of fibrillar collagen.
KPC-CDK1 cells: green, mCerulean.
ECM: magenta, SHG.
Related to Fig. 4.

Movie S6. Intravital monitoring of CDK1 accumulation in subcutaneous KPC tumors. *Related to Fig. 4.*

Movie S7. Intravital imaging of quantum dots circulating through tumor-associated vasculature and diffusing into tumor tissue upon priming with Fasudil. Panel 1: z-stack through KPC subcutaneous tumor injected with Quantum Dots. Green: KPC cells (mTurquoise2); magenta: Collagen (SHG); red: Quantum Dots. Panel 2: 3D representation of z-stack acquisition of Quantum Dot signal in subcutaneous KPC xenografts from mice treated with control or Fasudil. Panel 3: time series acquisition of Quantum Dots circulating through blood vessels and diffusing into tumor tissue of mouse treated with Fasudil. *Related to Fig. 4.*

Movie S8. Imaging of liver tissue with metastatic KPC cells expressing the CDK1 biosensor forming macrometastases and micrometastases.
Green: mCerulean KPC CDK1 metastatic cells; magenta: collagen I (SHG signal). *Related to Fig. 5.*

Movie S9. Time-lapse tracking of collective cell streaming on CDMs unprimed or primed with Fasudil. KPC cells were seeded on CDMs primed or unprimed with Fasudil (right panel), and cell movement was imaged over 62 hours. *Related to Fig. 7.*